

## MICROSTRUCTURE AND ELECTROCHEMICAL CHARACTERISTICS OF ELECTRODEPOSITED Zn-Ni ALLOY COATINGS

N. R. SHORT\*, WEN-HUA HUI\*\* AND J. K. DENNIS\*

\* *School of Engineering and Applied Science, Aston University,  
Birmingham, B4 7ET, UK*

\*\* *Department of Materials Science & Engineering, Stevens Institute of Technology,  
Hoboken, NJ 07030, USA.*

### Abstract

Electrodeposited Zn-Ni alloy coatings are of particular interest for improving the corrosion resistance of steel in a number of environments. Of particular interest is the relationship between composition, structure and corrosion rate. This paper firstly reviews the literature regarding composition-structure relationships of Zn-Ni electrodeposits and compares them with the equilibrium phase diagram. Secondly, research was carried out on a wide range of coatings which were produced in the laboratory and their structure and corrosion rates determined. It was found that unambiguous identification of phases from XRD data can be difficult. Maximum corrosion resistance of deposits is obtained at 12-13% Ni, with a  $\gamma$  phase structure and predomination of (600) and (411) reflections. Compatibility is important with regard to chromate conversion coatings.

*Key words* : Electrodeposits, ZnNi, Structure, Corrosion, Surfaces.

### 1. INTRODUCTION

Electrodeposited Zn-Ni alloy coatings are of particular interest for improving the corrosion resistance of automobile components<sup>1)</sup>, potential substitutes for cadmium electroplate<sup>2)</sup> and possible use in construction industry environments<sup>3)</sup>. Alloys containing about 10-15wt% Ni are found to offer the maximum corrosion resistance<sup>4)</sup>. A conversion coating is essential to achieve maximum corrosion protection and it is

now evident that there is a considerable synergistic effect between improvements found by the addition of alloying elements to the zinc and compatible conversion coating treatments<sup>4,5)</sup>. In addition paints may be applied to give a duplex coated steel and further corrosion protection.

Whilst alloy composition is a major factor in determining corrosion resistance of the coating, the phase constitution such as crystal structure and orientation is also important and in addition significant with regard to e.g. compatibility of

conversion coatings and adherence of paint films. Furthermore, the physical properties of the coating such as hardness and formability will also influence the range of applications. For instance as the Ni content in the deposit increases the microhardness increases whilst the interfacial shear stress decreases, so that poor formability results when the Ni content is 13%<sup>6)</sup>. The adhesion of paint films and their resistance to corrosion in scribe tests is greater for deposits with 11-14% Ni than those with 8-9% Ni<sup>7)</sup>.

Data for the Zn-Ni equilibrium phase diagram has been assessed and compiled in a number of publications<sup>8-11)</sup>. Phases found at ambient temperatures with their composition ranges and structures are given in Table 1. These compilations are generally consistent apart from the  $\gamma$  and  $\gamma_1$  phases, which in the most recent assessment<sup>11)</sup> is considered as a single phase field with composition limits of 14-24 wt% Ni. Thus the equilibrium phases at room temperature are<sup>11)</sup>: (a) zinc solid solution  $\eta$  with cph structure and maximum solubility of 0.2wt% Ni; (b) the  $\delta$  phase with a monoclinic structure and which occurs over a narrow composition range, 9-10 wt% Ni; (c) the  $\gamma$  phase with a structure closely related to  $\gamma$  brass although also described as orthorhombic and bcc like; (d) the  $\beta$  phase based on the stoichiometric compound ZnNi with CuAu structure (tetragonal or orthorhombic)

with composition limits of 45-52 wt% Ni; (e) solid solution  $\alpha$  fcc.

It is known that metastable phases may be deposited during the electroplating process and thus those present in electrodeposits may not be as predicted by the equilibrium phase diagram. A number of publications have been concerned with the structure of Zn-Ni electrodeposits<sup>6,12-19)</sup>. To aid comparison, the results of these investigations are shown schematically in Fig. 1 along with the composition limits as found in the equilibrium phase diagram. It is evident from this comparison that for a given Ni content the phase constitution can vary considerably. This presumably is a result of the different deposi-

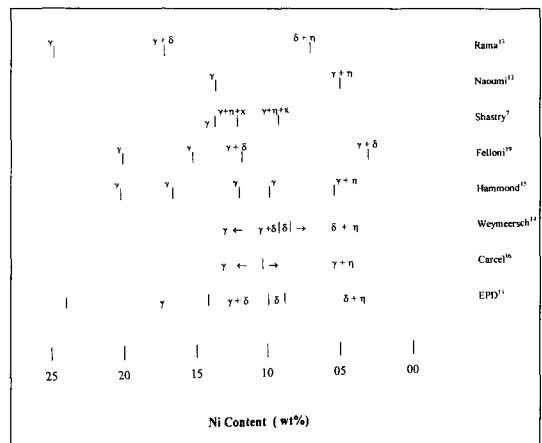


Fig. 1 Schematic diagram showing the phases present in a range of electrodeposited Zn-Ni alloys during different investigations. Composition limits from the equilibrium phase diagram (EPD) are included for comparison.

Table 1. Equilibrium Phases with Composition Ranges for the Zn-Ni System

(Ni wt.-%)						
$\alpha$	$\beta$	$\gamma_1$	$\gamma$	$\delta$	$\eta$	Ref.
74-100	47-55	22	12-16	9-10	0.2	Hansen <sup>8)</sup>
72-100	45-52	21-25	14-20	10-11	-	Brenner <sup>9)</sup>
71-100	45-52	-	14-24	9-10	0.2max	Nash <sup>11)</sup>

tion parameters used in the various investigations. For compositions around 12-13% Ni it can be seen that different investigators have shown that single ( $\gamma+\delta$ ) or ternary ( $\gamma+\delta+x$ ) phase fields may exist in the coatings. Other commercial operations e.g. paint curing, may involve annealing and if single ( $\gamma$ ) phases are present at compositions of 12-13% Ni (where a metastable state exists) then transformation to the  $\delta$  phase may occur<sup>20</sup>.

Work on zinc alloy coatings for protecting steel from corrosion in a wide range of environments has been carried out at Aston for over 15 years. The work presented in this paper concerns the relationship between structure/composition and corrosion resistance of a range of Zn-Ni alloy coatings.

## 2. EXPERIMENTAL

The Zn-Ni alloys were electrodeposited from an acid chloride bath having a composition of ZnCl<sub>2</sub> (60-90 g/l), KCl (180-220 g/l), H<sub>3</sub>BO<sub>3</sub> (25-35 g/l) and 0-20 ml/l additives. The pH, temperature and current density were 4.5-5.5, 30-40 °C and 2.0-8.0 A/dm<sup>2</sup> respectively. By changing the nickel content in the bath (added as NiCl<sub>2</sub>·6H<sub>2</sub>O) deposits were obtained with Ni contents between 2-92 wt.%. Structure was investigated at up to 92 wt.% and the coatings were ~20 μm thick. For corrosion studies coatings representing the more realistic commercial range, 22 wt.%, 12.5 μm were studied. Further samples which had been plated commercially and had a Ni content of 13.8% and were ~9.5 μm thick. Thick were in the as plated and chromated states.

Coating compositions of the plated layers were determined using energy dispersive x-ray analysis in the scanning electron microscope. X-ray diffraction (XRD) was used to obtain information on the phase structure. Plated samples were placed in a diffractometer and the operating conditions used were CuK $\alpha$ , 40kV, 30mA.

The commercially plated samples were analysed by X-ray photoelectron spectroscopy (XPS). Mg K $\alpha$  radiation was used as the excitation source. General information was obtained from wide scan survey spectra whilst more detailed knowledge was obtained from high resolution spectra of Zn 2p<sub>3/2</sub>, Ni 2p<sub>3/2</sub>, O<sub>1s</sub> and Cr 2p<sub>3/2</sub> peaks. Analyses were carried out after various times of sputtering to obtain depth profiles of these elements.

The electrochemical behaviour of the samples was monitored on a weekly basis by measuring the polarisation resistance and then calculating the corrosion rate. Further details of the procedures are given elsewhere<sup>4</sup>. Salt spray tests were carried out using a neutral 5% solution of NaCl and exposed in accordance with BS 5466.

## 3. RESULTS AND DISCUSSION

### 3.1 Structure of Coatings

X-ray diffraction data for the range of laboratory Zn-Ni alloy electrodeposited coatings are given in Table 2. Values of  $d_{hkl}$  (Å) were calculated using the diffraction angle  $\theta$  and a value of  $\lambda=1.5418$  Å.  $I/I_1$  represents the relative diffraction strength. Using these values the corresponding plane indices (hkl) and phases were

Table 2. X-ray Diffraction Data for Laboratory Zn-Ni Alloy Electrodeposits

Ni Content (wt. %)	$2\theta(^{\circ})$	d <sub>hkl</sub> (Å)	I/I <sub>1</sub>	Plane Index (hkl)	Phase
2.1	38.94	2.31	82	(100) or (004)	$\eta$ or $\delta$
	43.20	2.09	100	(101) or (411)	$\eta$ or $\delta$
	70.56	1.33	50	(110) or (630)	$\eta$ or $\delta$
7.0	36.44	2.46	21	(002)	$\eta$
	38.98	2.31	7	(100) or (004)	$\eta$ or $\delta$
	43.14	2.10	100	(101) or (411)	$\eta$ or $\delta$
	70.74	1.33	11	(110) or (630)	$\eta$ or $\delta$
10.2	62.38	1.49	100	(600)	$\gamma$
13.8	43.02	2.10	34	(411)	$\gamma$
	62.56	1.48	100	(600)	$\gamma$
17.6	42.8	2.11	20	(411)	$\gamma$
	62.42	1.49	100	(600)	$\gamma$
21.5	63.08	1.47	100	(600)	$\gamma$
29.3	35.26	2.54	100	?	?
	62.70	1.48	50	(600)	$\gamma$
47.3	35.54	2.52	100	?	?
	79.90	1.20	22	(642)	$\gamma$
56.7	35.50	2.53	42	?	?
	45.00	2.01	38	(101)	$\beta$
	52.50	1.74	75	(200)	$\alpha$
	56.70	1.62	29	(002)	$\beta$
	79.00	1.21	100	(112)	$\beta$
	86.50	1.13	8	(211)	$\beta$
	96.00	1.04	100	(202)	$\beta$
64.8	43.92	2.06	100	(111)	$\alpha$
	51.26	1.78	21	(200)	$\alpha$
	73.04	1.29	16	(444)	$\beta$
	75.60	1.26	19	(220) or (112)	$\alpha$ or $\beta$
69.5	44.42	2.04	100	(111)	$\alpha$
79.1	44.20	2.05	100	(111)	$\alpha$
	51.66	1.77	29	(200)	$\alpha$
91.8	44.30	2.04	100	(111)	$\alpha$
	51.72	1.77	11	(200)	$\alpha$

determined by comparing with the Joint Committee on Powder Diffraction Data<sup>21)</sup> on microfiche. Owing to the similarity in reflections for the various structures it is somewhat difficult to identify phase fields unambiguously. Thus at coating contents of 2.1 and 7.0% Ni, the phase present could be either  $\eta$  or  $\delta$  or probably both.

For coatings with compositions in the range 10.2 to 21.5% Ni the  $\gamma$  phase appears to predominate. Values of relative intensity for the diffraction peaks showed that the coatings have a strong tendency for preferred orientation, the patterns being dominated by (600) reflections. In two of the alloys 13.8 & 17.6% significant (411) reflections were also observed. At Ni concentrations of 29.3, 47.3 & 56.7% a reflection is present,  $d_{hkl} = 2.53 \text{ \AA}$ , which does not match any reflection in the files and the reason for its presence remains to be resolved. At Ni contents of 56.7 and > 64.8% the  $\beta$  and  $\alpha$  phases predominate respectively and the phases found are those to be expected from the equilibrium phase diagram.

Diffraction data for the commercial Zn-Ni alloy electrodeposit (13.8% Ni) are given in Table 3. As with the laboratory produced deposit the  $\gamma$  phase appears to predominate. However, in this case the (411) reflections were prominent in the pattern although other reflections, (600) & (532), were present.

### 3.2 Corrosion Behaviour

The corrosion behaviour of a range of coatings with Ni contents up to 22% was investigated using a neutral salt spray test and linear polarisation for corrosion currents. The changes in time to red rust with Ni content are shown in Fig. 2. It can be seen that significant improvement in corrosion resistance is obtained when the coatings contain 10-15% Ni. Optimum corrosion resistance is obtained when the Ni content is around 12-13%.

The electrochemical measurements revealed additional information in that initially the corrosion rates for all samples were about the same and it is only after about 10 days that the effect of different Ni contents become evident<sup>4)</sup>. Fig. 3 shows the change in corrosion rate with time for a laboratory produced coating with 12.4% Ni and the commercially produced coating with

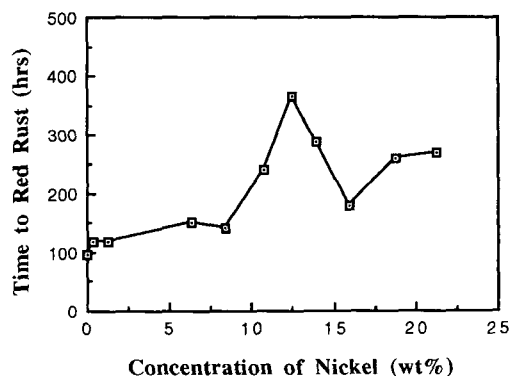


Fig. 2 Effect of Ni contents on time to red rust, samples  $12.5\mu\text{m}$  thick.

Table 3. X-ray Diffraction Data for the Commercial Zn-Ni Alloy Electrodeposit

Ni Content (wt. %)	$2\theta(^{\circ})$	$d_{hkl}$ ( $\text{\AA}$ )	$I/I_1$	Plane Index (hkl)	Phase
13.8	43.0	2.10	100	(411)	$\gamma$
	62.5	1.49	6	(600)	$\gamma$
	78.5	1.22	13	(552)	$\gamma$

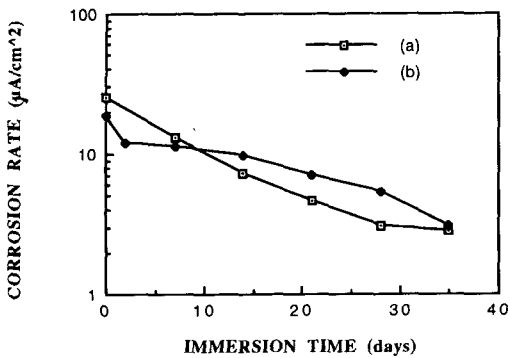


Fig. 3 Change in corrosion rate with time for (a) laboratory produced coating, 12.4% Ni, (600) reflections dominate. (b) commercial produced coating, 13.8% Ni, (411) reflections dominate.

13.8% Ni. Corrosion rates for both coatings are very similar and diminish with time. During this period it has been found<sup>4)</sup> that preferential dissolution of Zn takes place with Ni enrichment of the coating surface. If the average corrosion rate (taken between 20-30 days) is plotted against Ni content for a range of coatings, the trends found are as shown in Fig. 4. This variation in corrosion rate with coating composition mirrors the results shown in Fig. 2 i.e optimum corrosion resistance is obtained when the Ni content is around 12-13%.

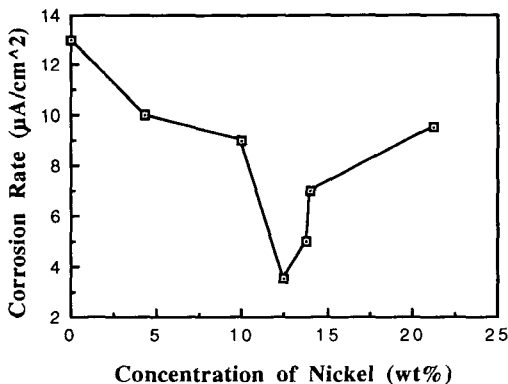


Fig. 4 Effect of Ni content on corrosion rate.

This figure of 12-13% for optimum corrosion resistance correlates with coatings having a  $\gamma$  phase type of structure. However, since the laboratory and commercial coatings have different preferred orientations, (600) and (411) respectively, yet show little difference in corrosion rate (Fig. 3), this latter factor may not be crucial in determining corrosion resistance.

The corrosion potentials, Fig. 5, for alloys containing up to 10% Ni were generally very similar to those of pure Zn and remained at low active values of around -1000 to -1100mV (SCE). For alloys with > 10% Ni the corrosion potential increases during the first 10-20 days and for a Ni concentration of 14% reached values of around -650mV. This increase would appear to reflect Ni enrichment of the surface as much as a phase change. However, since these potentials were less than that of iron in similar solutions,  $\sim$ -570mV, a level of sacrificial protection should still occur.

### 3.3 Surface Analysis

Fig. 6 shows the composition gradients at the surface of the non-chromated Zn-13.8%Ni alloy coating. It can be seen that the surface was essentially zinc oxide as might be predicted from

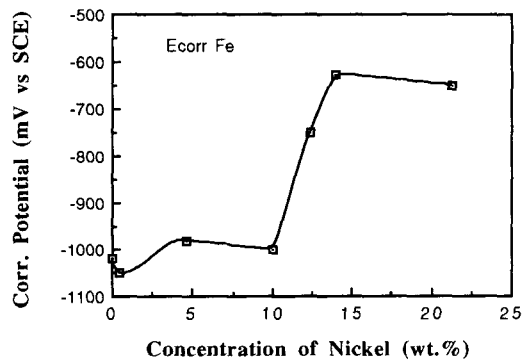


Fig. 5 Effect of Ni content on corrosion potentials.

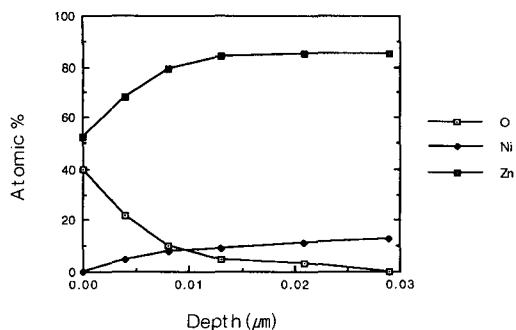


Fig. 6 Surface analysis of non-chromated Zn-13.8% Ni alloy coating.

thermodynamic considerations. Thus the surface is not directly passivated by the formation of NiO. Fig. 6 also shows that this surface layer, is only about 10nm thick and would be quickly removed in a corrosive environment. This is in keeping with the discussion above where it is considered that corrosion resistance is dependent on preferential dissolution of zinc and the formation of a Ni rich surface layer thus forming a protective barrier. The  $\gamma$  phase in some way facilitates this process, but only at Ni contents at the lower end of its composition range i.e 10-15%.

Increased corrosion rates at Ni contents below 10% are relatively easy to understand, since a two phase structure e.g. ( $\eta + \delta$ ) or ( $\eta + \gamma$ ) is likely to exist. This facilitates establishment of local cells and hence preferential attack of the less noble phase. In contrast increased corrosion rates at Ni contents above 15% are less easy to understand since a single phase field still prevails. It may be that selective dissolution of zinc and formation of a barrier layer is also accompanied by large surface stresses which in turn facilitate the dissolution mechanism or fracture of the protective film<sup>22</sup>.

In the case of the chromated sample, Fig. 7,

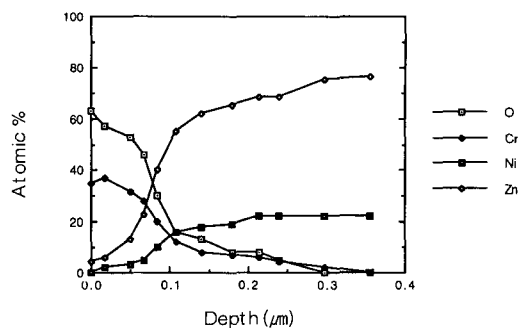


Fig. 7 Surface analysis of chromated Zn-13.8% Ni alloy coating.

chromium oxide was predominant, again as expected from thermodynamic considerations. Furthermore, chromium is mainly present as Cr (III) rather than Cr (VI) suggesting that protection is given by a barrier layer ( $\sim 0.1 \mu\text{m}$ ) rather than inhibitive action of soluble ions. The fact that the coatings may be dominated by (600) or (411) planes may be of importance in this respect. It is known that chromate films form best on (100) planes<sup>23</sup> in the case of pure zinc crystals. However, special conversion coatings are required for alloy layers and not all chromating processes are equally effective in this manner<sup>4</sup>. It is finding ones compatible with the phase composition and structure of the alloy layer that is the key to good corrosion performance. A similar argument would apply to the application of organic films although an additional problem would arise if the applied films are baked when the possibility of transformation from the metastable to equilibrium phase may take place.

#### 4. CONCLUSIONS

1) Interpretation of X-ray diffraction data and unambiguous identification can be difficult

as a result of similar reflections for the different phases.

2) Maximum corrosion resistance of Zn-Ni alloy electrodeposits occurs when the structure consists of the  $\gamma$  phase and either the (600) or (411) reflections dominate.

3) Optimum corrosion resistance (12–13% Ni) is obtained by the formation of a barrier layer which is particularly stable for this phase structure and narrow composition range.

4) Suitable compatibility is important with regard to chromate conversion coatings.

## 5. ACKNOWLEDGEMENTS

We would like to acknowledge contributions made in earlier years to our research programme on zinc alloy electrodeposits by Drs. A. Abibsi & S. Zhou which has helped in the writing of this paper.

## REFERENCES

1. S.A. Watson, *Trans. IMF*, 79, 28, (1992)
2. K.R. Baldwin and C.J.E. Smith, *Trans. IMF*, 74, 202, (1996)
3. N.R. Short and J.K. Dennis, *Trans. IMF*, 75, 47, (1997)
4. N.R. Short, A. Abibsi and J.K. Dennis, *Trans. IMF*, 67, 78, (1989)
5. A. Abibsi, N.R. Short and J.K. Dennis, *Trans. IMF*, 69, 45, (1991)
6. S.H. Hsieh, C.S. Lin and F.T. Chen, *China Steel Technical Rept. No. 10*, 43, (1996).
7. C.R. Shastry, *Proc. Soc. Auto. Eng.*, 250, 239, (1991)
8. M. Hansen, *Constitution of Binary Alloys*, McGraw-Hill, New York, 1958
9. A. Brenner, *Electrodeposition of Alloys, Principles and Practice*, Academic Press, New York, 1963.
10. A.J. Morton, *Acta Metallurgica*, 27, 863–867, (1979)
11. P. Nash and Y. Y. Pan, in *Binary Alloy Phase Diagrams*, Ed. T. B. Massalski, Am. Soc. Metals, (1986), pp.1772–1774.
12. R. Naoumi, H. Nagasaki, Y. Foboh and A. Shibuya, *SAE Technical Paper No. 820332*, Detroit, February 22–26, (1982)
13. T.L. Rama Char and S.K. Panikkar, *Electroplating & Metal Finishing*, 13, 405, (1960).
14. Weymeersch, L. Renardk, J.J. Conreur, R. Winand, M. Jorda and C. Pellet, *Plating and Surface Finishing*, 73, 68–71 (1986)
15. L. Hammond and D. Wright, *Mat. Sci. Forum*, 133–136, 501, (1993)
16. A.C. Carcel and C. Ferrer-Gimenez, *Rev. Metal. Madrid*, 29, 83 (1993)
17. K. Kondo, M. Yokoyama and K. Shinohara, *Electrochem. Soc. Proc.* 94–31, 238 (1994)
18. P.L. Hansen and C.Q. Jessen, *Scripta Metallurgica*, 23, 1387 (1989)
19. L. Felloni, R. Fratesi, E. Quadrini and G. Roventi, *J. App. Electrochem.*, 17, 574 (1987)
20. P.L. Hansen and C.Q. Jessen, *Scripta Metallurgica*, 23 (1989) 1387
21. Joint Committee on Powder Diffraction Data. *Powder Diffraction File of Inorganic Phases*, Ed. Int. Centre for Diffraction Data, 1990
22. K.E. Heusler, *Corrosion Science*, 39 1177 (1997)
23. D.K. Kim and H. Leidheiser, *Metall. Trans.* 9B, 581 (1978)